ANL-6055
Metals, Ceramics,
and Materials
(TID-4500, 17th Ed.)
AEC Research and
Development Report

ARGONNE NATIONAL LABORATORY
9700 South Cass Avenue
Argonne, Illinois

THE URANIUM-RICH END OF THE URANIUM-ZIRCONIUM SYSTEM

by

S. T. Zegler

Metallurgy Division

Final Report - Metallurgy Program 3.1.3

Parts of this report have appeared in the following Metallurgy Division Reports:

ANL-4923	p. 87	July-September 1952
ANL-4966	pp. 34-35	October-December 1952
ANL-5097	pp. 45-49	April-June 1953
ANL-5234	pp. 51, 53-57	October-December 1953
ANL-5257	pp. 33-35	January-March 1954
ANL-5338	pp. 59-61	April-June 1954
ANL-5423	pp. 63-66	October-December 1954
ANL-5439	pp. 30-32	January-March 1955
ANL-5489	pp. 45, 47-50, 51	July-September 1955
ANL-5623	pp. 58-63	April-June 1956
ANL-5643	pp. 42-45	July-September 1956
ANL-5975	p. 53	March 1959

February 1962

Operated by The University of Chicago
under
Contract W-31-109-eng-38

DISCLAIMER

TABLE OF CONTENTS

LIST OF FIGURES

LIST OF TABLES

THE URANIUM-RICH END OF THE URANIUM-ZIRCONIUM SYSTEM

by

S. T. Zegler

ABSTRACT

The uranium-rich end of the uranium-zirconium alloy system has been reinvestigated. The solubilities of zirconium in alpha and beta uranium were found to be 0.21 weight per cent at 662°C and 0.41 weight per cent at 693°C, respectively. The monotectoid decomposition of γ_1 at 693°C and the eutectoid decomposition of β at 662°C were confirmed. For alloys containing less than 150 ppm of oxygen by weight, the gamma$_1$ plus gamma$_2$ phase region boundaries have been located at 4.5 weight per cent and 22.0 weight per cent zirconium at the monotectoid temperature. Data are given which indicate that oxygen concentrations ranging from 160 to 355 ppm by weight have a marked effect on phase relations in the area of the gamma$_1$ plus gamma$_2$ phase region.

INTRODUCTION

The uranium-zirconium alloy system has been studied and phase diagrams have been reported by a number of investigators.[1-14] The various reported diagrams have recently been reviewed by Rough and Bauer.[1] Kaufman,[2] Peterson,[3] and Buzzard, Liss, and Fickle[4] early established the principal features of the system. The high-zirconium end of the system has recently been determined with greater accuracy by Bauer, Rough et al.[5,6] Their interpretation of the portion of the system extending from 35 to 100 weight per cent zirconium, which is in fair agreement with those of others,[7,8,9] and also their finding that the delta peritectoid reaction occurs at 607°C, is incorporated in the phase diagram shown in Figure 1. The high-uranium end of the system has been studied most recently by Rough and coworkers at Battelle[1] and by Summers-Smith.[14] Their reported phase diagrams are reproduced in Figures 2 and 3, respectively. Their findings are of particular significance in establishing the existence of a gamma$_1$ plus gamma$_2$ phase region not previously noted by others. Their results differ, however, as to the temperature and compositional limits of the two-phase region and also as to

the solubility limits of zirconium in alpha and beta uranium and the temperature of the alpha-beta transformation in the alloys. The present investigation of the high-uranium end of the system was initiated to determine these features of the diagram with greater accuracy.

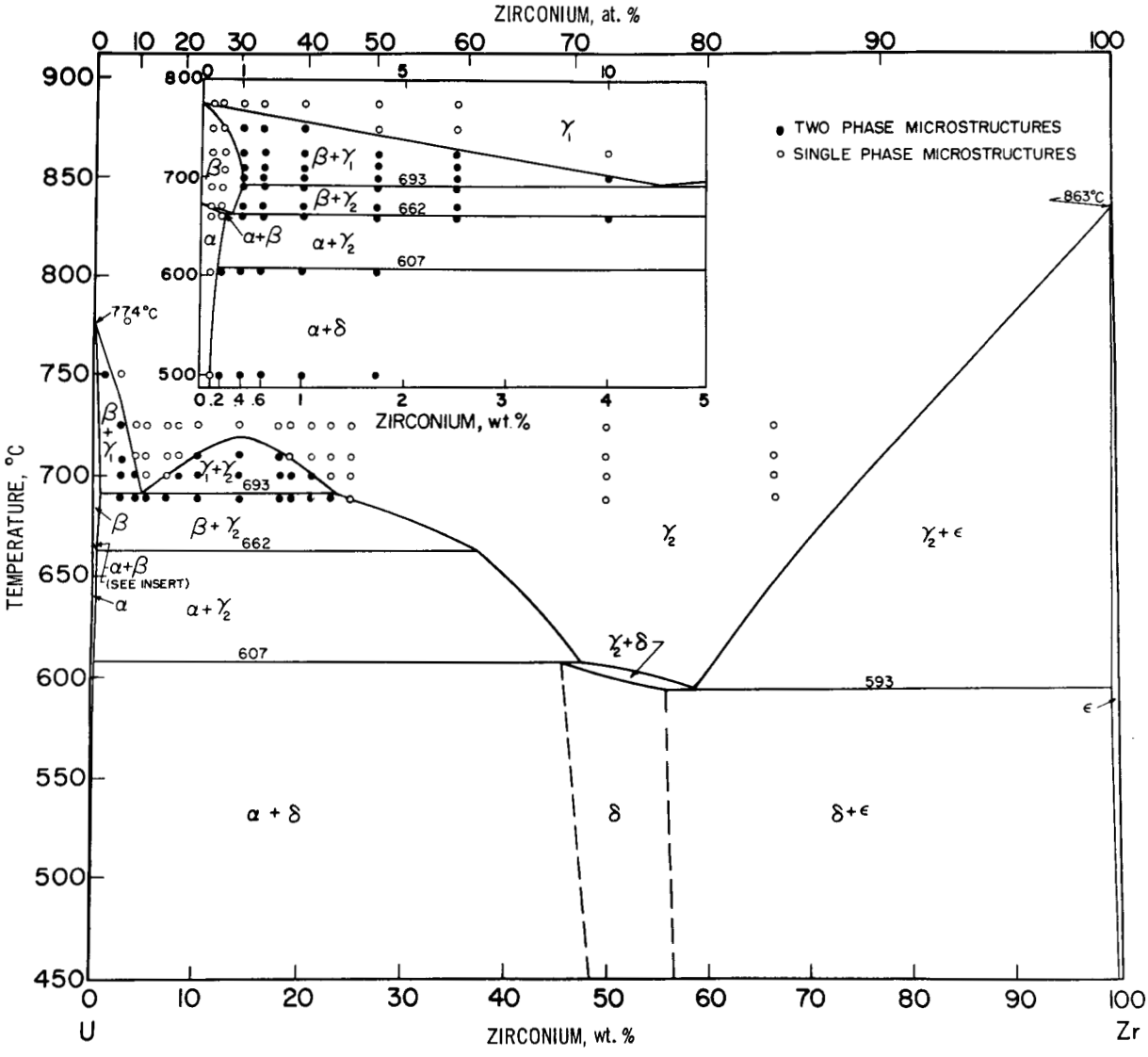

Figure 1. Equilibrium Phase Diagram of Uranium-Zirconium Alloy System. Macro No. 27159.

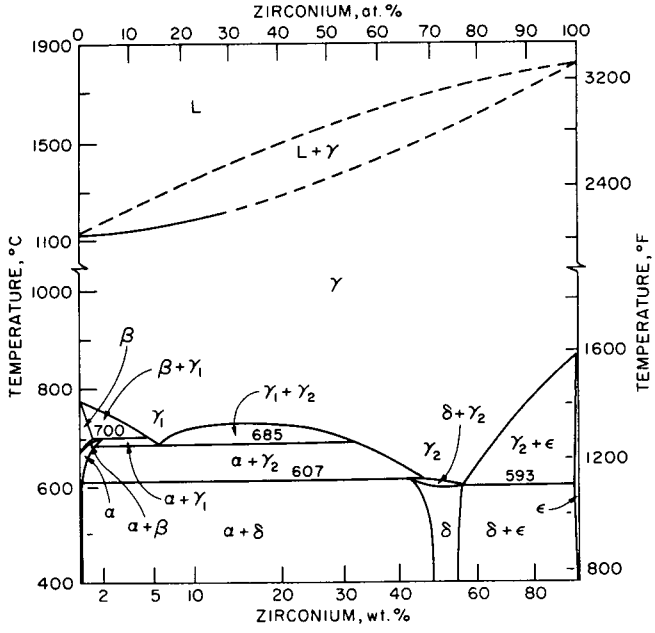

Figure 2. Equilibrium Phase Diagram of Uranium-Zirconium Alloy System According to Rough and Bauer,[1] Macro No. 108-4375.

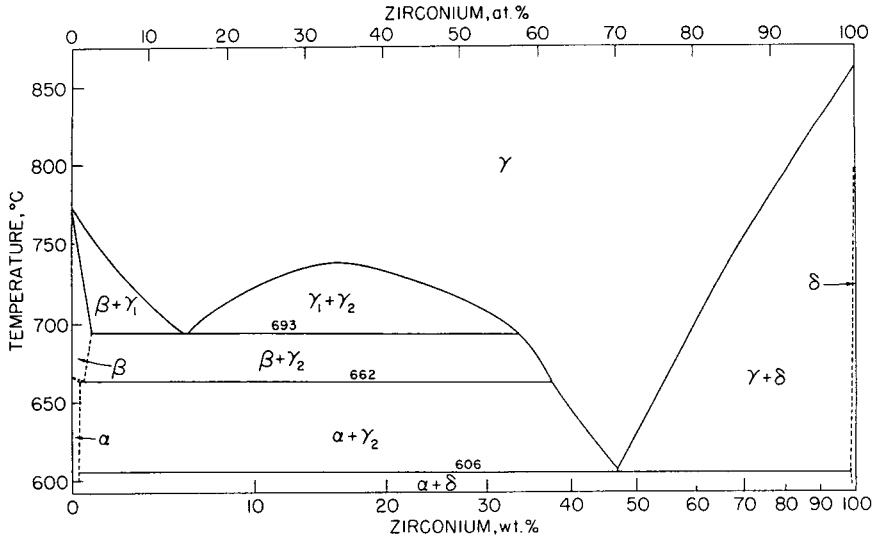

Figure 3. Equilibrium Phase Diagram of the Uranium-Zirconium Alloy System According to Summers-Smith.[14] Macro No. 108-4376.

EXPERIMENTAL PROCEDURE

Preparation of Alloys

Preliminary to the preparation of the alloys used in this investigation a study was made of general melting and casting practices for producing alloys containing up to 2 w/o Zr having uniform composition and high purity. Several ingots of alloys within this composition range were made from high-purity uranium crystals, prepared electrolytically, and small turnings of zirconium crystal bar. The alloys were induction melted in thoria or magnesia crucibles at temperatures up to 1400°C and at furnace pressures of the order of 2×10^{-5} mm of mercury. In some cases the melts were slow-cooled in the crucibles; others were bottom poured into water-cooled copper molds. Melting at temperatures just above liquidus temperatures followed by slow cooling in the crucibles was found to result in extensive segregation of zirconium at the tops of the ingots, due to flotation of zirconium to the surface during melting. Melting at 1400°C followed by pouring into water-cooled copper molds was found to be most effective for producing ingots exhibiting little or no zirconium segregation. Substantial pickup of nitrogen, in amounts up to 750 ppm, and its segregation also at the tops of the ingots was also encountered. Microexamination of annealed specimens cut from the ingots indicated, as will be shown later, that, in amounts greater than 65 ppm, nitrogen markedly influences microstructures. Thus for studies of phase relations up to 2.5 w/o Zr, only alloys containing less than this amount of nitrogen were used. The alloys were generally obtained by selecting portions of the bottoms of ingots.

For the phase diagram studies described in this report 34 uranium-zirconium alloys containing up to 67.3 weight per cent zirconium were prepared from 99.98 per cent pure uranium and 99.93 per cent pure Grade II zirconium. The nominal compositions of the alloys, calculated from the weights of uranium and zirconium added for melting, are given in column 2 of Table I.

Alloys Nos. 1 through 7 were melted in vacuum by induction heating in magnesia crucibles and cast into water-cooled copper molds. The cast ingots, having a $1\frac{3}{4}$-in. diameter, were rolled in air, first to $1\frac{1}{2}$ in. in diameter at 800°C and next to $\frac{1}{2}$ in. in diameter at 600°C. After rolling, chemical and spectrographic analyses were obtained at the end and mid-length positions of rods selected for study. The averaged results of the analyses are given in columns 3 through 9 of Table I. In all cases, deviations from the average zirconium values were small; less than 0.01 weight per cent zirconium for alloys Nos. 1 through 3 and less than 0.06 weight per cent zirconium for alloys Nos. 4 through 7. Subsequently, the alloys were given a homogenization heat treatment for 2 hr at 1000°C

and quenched in Wood's metal. For the heat treatment the rods were cut into discs, $\frac{1}{8}$ in. in thickness. Heating and quenching of the discs were done within an evacuated furnace operating at a dynamic pressure of 2×10^{-5} mm of mercury.

Table I

COMPOSITIONS OF URANIUM-ZIRCONIUM ALLOYS

Alloy No.	Nominal w/o Zr	Analyzed w/o Zr	O (ppm)	N (ppm)	C (ppm)	Fe (ppm)	Mo (ppm)	Si (ppm)
1	0.1	0.09		22	7	40	30	40
2	0.2	0.21		26	6	30	20	40
3	0.4	0.41		26	7	100	20	100
4	0.6	0.70		16	8	20	20	20
5	1.0	1.07		24	15	70	20	40
6	1.7	1.60		20	20	20	700	20
7	2.5	2.30		23	11	20	500	20
8	4.0		93	69				
9	5.0	4.7	110	65				
10	6.5							
11	6.9		28	68				
12	8.0		93	112				
13	9.0	8.8	20	13				
14	10.0		44	46				
15	11.0		22	73				
16	11.4							
17	13.0	13.0	48	10		30	20	40
18	14.0		125	26				
19	15.0		51	86				
20	17.0		53	74				
21	19.0		75	149				
22	21.0		65	57				
23	21.3							
24	23.0	22.8	68	10		50	20	60
25	25.0		71	23				
26	25.2		120	10				
27	27.0		70					
28	32.0	32.0	134	35		100	20	60
29	37.9		85	66				
30	43.7		150	10				
31	50.0		120	47				
32	55.5		150	116				
33	61.2		140	72				
34	67.3		100	59				

Alloys Nos. 8 through 34 were in the form of buttons, weighing approximately 40 gm each, prepared by arc melting and casting in an argon-helium atmosphere in a furnace previously described.[15] Chemical homogeneity was attained by remelting the buttons six times. Chemical

analyses for zirconium were obtained on a representative number of the cast buttons and are given in Table I. In all cases, values obtained from analyses were in agreement with nominal values to within ± 0.3 weight per cent zirconium. Except where otherwise noted, nominal values expressed in weight per cent are used throughout this report. Chemical analyses for oxygen and nitrogen were done on most of the alloys and are given in Table I. Concentrations of each element did not exceed 150 ppm. The highest concentrations of oxygen and nitrogen occurred most often in the alloys having the highest zirconium contents. Spectrographic analyses for iron, molybdenum, and silicon were done on only three of the cast alloys (see Table I).

Heat Treatment and Metallography

Equilibrium phase relations were determined chiefly from metallographic studies of specimens annealed for periods up to 2 weeks at the temperatures shown in Figure 1 and water quenched. Prior to all annealing treatments the specimens, approximately $\frac{1}{8}$ in. in thickness, were cold pressed to 10 per cent reduction in thickness to promote diffusion at the annealing temperatures. Annealing treatments of alloys containing up to 2.5 per cent zirconium were conducted with the specimens wrapped in tantalum foil and sealed in Vycor capsules that had been evacuated at room temperature to a pressure of 2×10^{-6} mm of mercury. Specimens of alloys containing greater concentrations of zirconium were annealed in capsules which, after evacuation, were filled with argon gas to a pressure amounting to a fraction of one atmosphere at room temperature. The use of pressurized capsules for annealing the higher zirconium alloys was found from initial studies to be necessary to avoid excessive contamination by oxygen and nitrogen. Quenching after annealing was done by breaking the capsules under water.

For microexamination, the specimens were mounted in Bakelite, ground on water wheels through No. 600 paper, and polished on cloth wheels through No. 1 diamond paste. Specimens of alloys containing up to approximately 14 per cent zirconium were then electrolytically polished and etched in a solution of 8 parts phosphoric acid, 5 parts ethylene glycol, and 5 parts ethyl alcohol. Specimens of higher zirconium alloys were electrolytically polished in a solution of 10 per cent perchloric acid and 90 per cent acetic acid, and then etched in a warm aqueous solution containing 50 per cent nitric acid and 5 per cent hydrofluoric acid.

X-ray Diffraction

Diffraction studies were made of powders filed from the annealed specimens described above and also of small needles, approximately $\frac{1}{32}$ in. in diameter and $\frac{3}{8}$ in. long, which were annealed in the same manner as that described above. Patterns were obtained with a 114.6-mm DeBye-Scherrer camera and filtered Cu K-α radiation.

Thermal Analysis

Thermal arrest data were obtained for a 1.0 per cent zirconium alloy (Alloy No. 5) on heating and cooling between 625°C and 825°C at rates varying from 0.5°C to 1.5°C per minute. Heating and cooling rates were controlled by the differential thermocouple method. Arrest temperatures were determined with a calibrated platinum-rhodium thermocouple placed within a small drill hole in the specimen. The specimen was approximately $\frac{3}{8}$ in. in diameter and $1\frac{1}{2}$ in. long.

RESULTS AND DISCUSSION

The uranium-rich end of the uranium-zirconium system as determined in this investigation is shown in Figure 1. The existence at high temperatures of a broad single-phase field of body-centered cubic gamma solid solution, found earlier by others,[1-4,14] was confirmed in the present work from correlation of X-ray diffraction and metallographic data. Diffraction patterns showed that the gamma solid solution containing up to approximately 14 per cent zirconium transforms martensitically to alpha uranium upon water quenching. Microstructurally, the martensitic alpha structures of alloys containing up to approximately 2 per cent zirconium are characterized by a "veining" of parent gamma grain boundaries, as seen in Figure 4a. The cause of the veining was not determined. With zirconium in excess of 2 per cent, martensitic structures appear acicular, as seen in Figure 4b. In the preliminary study previously described, the acicular product was also observed in a nominal U-1.0 w/o Zr alloy which contained from 65 to 110 ppm of nitrogen. It was not observed, however, at nitrogen concentrations of 24 ppm or less. The transition from veined to acicular microstructures with either increasing zirconium or nitrogen concentrations is interpreted to be due possibly to an alteration in the mode of the martensitic reaction.

Diffraction patterns of alloys containing from 14 to 30 per cent zirconium quenched from the gamma phase field show the presence of alpha uranium and the low-temperature delta phase. As judged from diffraction line intensities, the martensitic reaction is gradually supplanted by the transformation of gamma to the delta phase as the zirconium content increases. Comparison of Figures 4c and 4d illustrates the microstructural change that occurs as the proportion of the delta phase increases. The microstructure shown in Figure 4c for the U-14.0 w/o Zr alloy is interpreted to be a mixture of martensitic alpha and a small amount of delta. The microstructure of the U-21.0 w/o Zr alloy in Figure 4d is essentially all delta phase supersaturated with uranium. The second-phase particles apparent in the microstructure are inclusions extraneous to the system. Diffraction patterns of quenched alloys containing from 30 to 67 per cent zirconium show the retention of body-centered cubic gamma in a metastable condition. Figure 4e typifies the coarse grain microstructures of alloys consisting of retained gamma.

U-0.6 w/o Zr

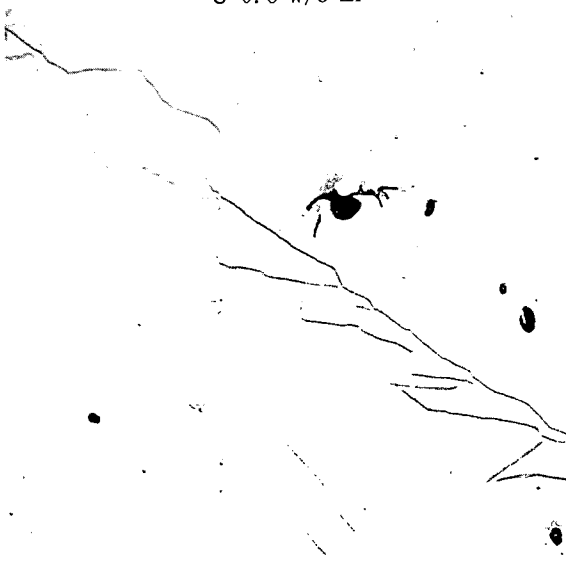

a. Veined martensitic alpha. Etchant: Phosphoric Acid. Micro No. 14808.

U-2.5 w/o Zr

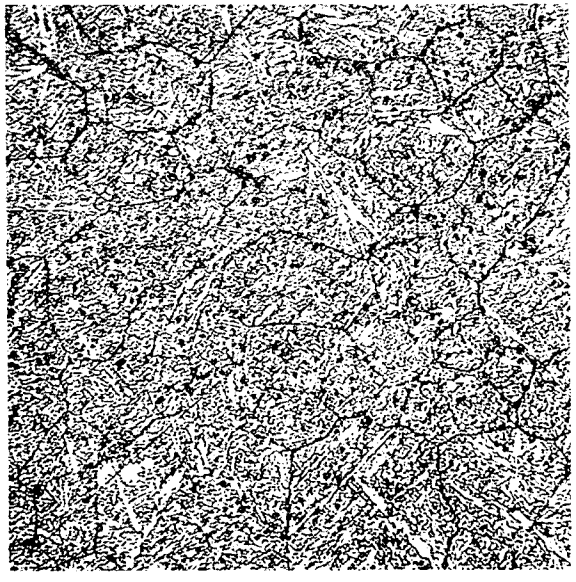

b. Acicular martensitic alpha. Etchant: Phosphoric Acid. Micro No. 16122.

U-14.0 w/o Zr

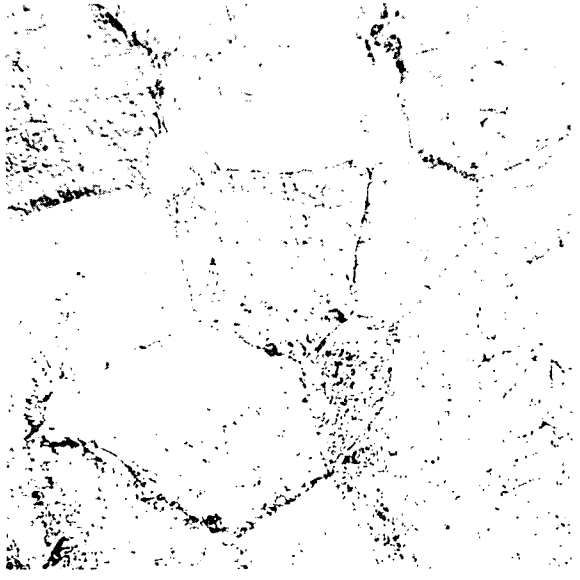

c. Mixture of martensitic alpha plus small amount of delta. Etchant: Phosphoric Acid. Micro No. 25139.

U-21.0 w/o Zr

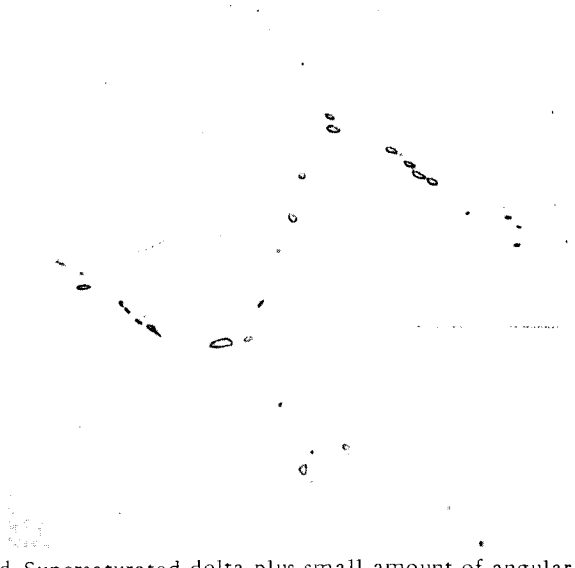

d. Supersaturated delta plus small amount of angular inclusions. Etchant: Perchloric-Acetic Acids. Micro No. 25140.

U-43.7 w/o Zr

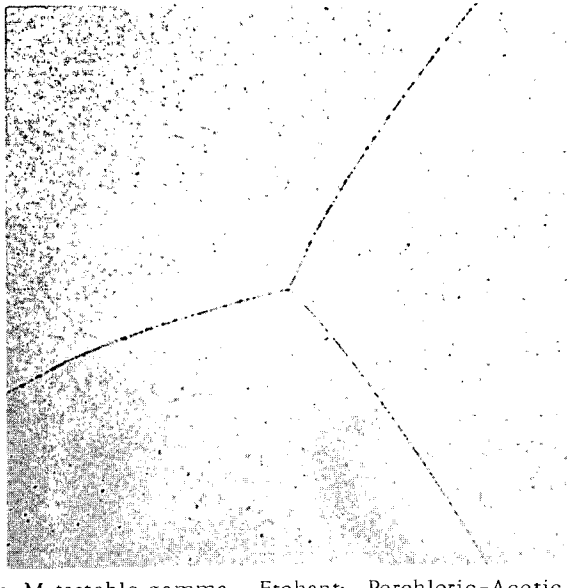

e. Metastable gamma. Etchant: Perchloric-Acetic Acids. Micro No. 21314.

Figure 4

Microstructures of Gamma-quenched Uranium-Zirconium Alloys. (All alloys annealed 1 week at 750°C and water quenched.

All photomicrographs taken at 500X with bright field illumination.

The hardness of alloys quenched from 750°C is plotted as a function of the zirconium content in Figure 5. It is clear that the retention of gamma in the higher zirconium alloys results in low hardness.

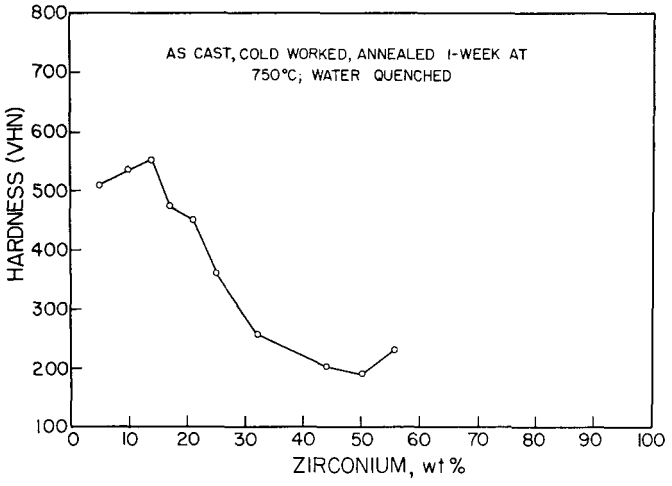

Figure 5. Hardness of Gamma-quenched Uranium-Zirconium Alloys. Macro No. 27160.

Solubility of Zirconium in Alpha and Beta Uranium

The disappearing-phase technique was employed for determining the solubility of zirconium in alpha and beta uranium. The results of the studies are plotted in Figure 1. Alloys annealed within the single-phase alpha and beta phase regions showed only small amounts of angular primary inclusions, as seen in Figures 6a and 6d. The inclusions, considered to be carbides of either uranium or zirconium, were not dissolvable even upon heat treatment for times up to 64 hr at 1000°C. Microstructures of alloys annealed within the alpha plus delta, alpha plus gamma$_2$, and beta plus gamma$_2$ regions are illustrated in Figures 6b, c, e, and f. In all cases, the minor phases appear as fine spheroidal particles, easily distinguishable from the angular primary inclusions. Identification of the minor phases by X-ray diffraction was not possible except in alloys containing 10 per cent zirconium or greater. In Figure 7 are photomicrographs of alloys annealed within the beta plus gamma$_1$ region. In alloys containing up to approximately 1.0 per cent zirconium and annealed at temperatures in the range from 700°C to 725°C, the martensitic product of the gamma$_1$ has very fine grain size, precluding resolution of its acicular appearance at ordinary magnifications. However, in alloys of higher zirconium concentration annealed at the same temperatures, the acicular character of the product is clearly defined, as is seen in Figure 9a. The acicular character of the product is also resolvable in alloys of 0.41, 0.65 and 1.0 per cent zirconium annealed at 750°C as shown in Figures 7d through 7f. X-ray diffraction patterns of alloys quenched from within the single-phase beta and two-phase beta plus gamma$_1$ or beta plus gamma$_2$ regions show only alpha uranium.

U-0.1 w/o Zr 500°C

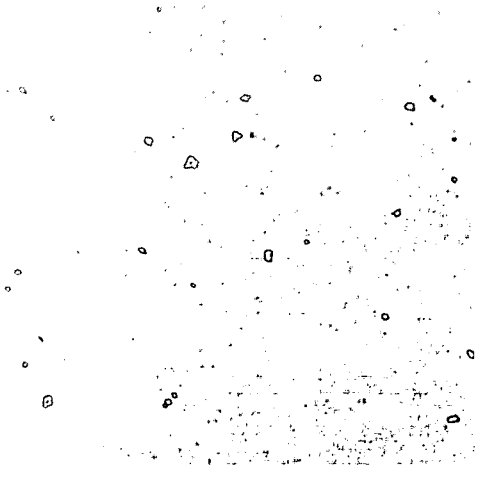

a. Alpha plus angular inclusions. Micro No. 14946.

U-0.2 w/o Zr 605°C

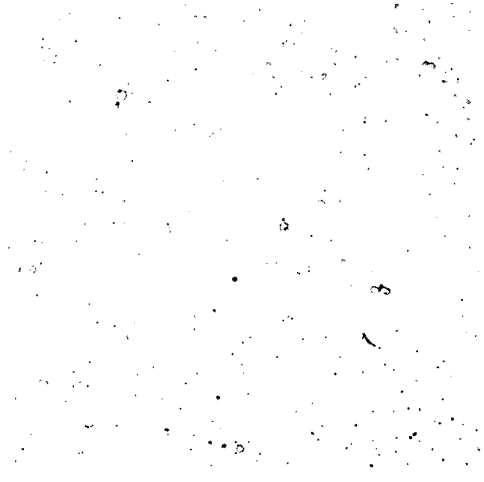

b. Alpha plus very fine delta particles. Micro No. 16743.

U-0.4 w/o Zr 605°C

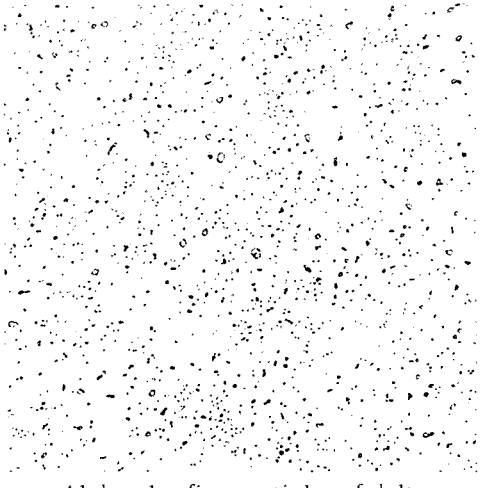

c. Alpha plus fine particles of delta. Micro No. 16744.

U-0.2 w/o Zr 660°C

d. Alpha plus small amount of inclusions. Micro No. 16705.

U-0.4 w/o Zr 660°C

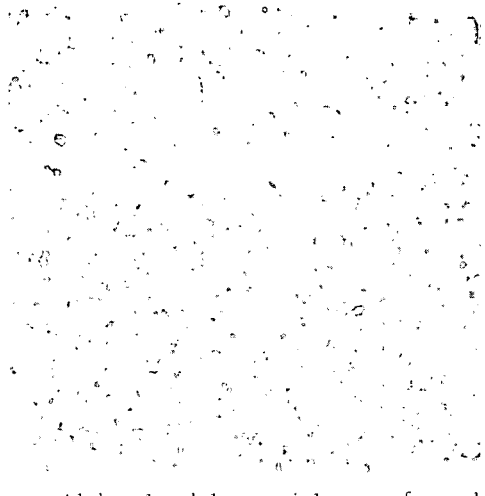

e. Alpha plus delta particles transformed from gamma2. Micro No. 16707.

U-0.6 w/o Zr 670°C

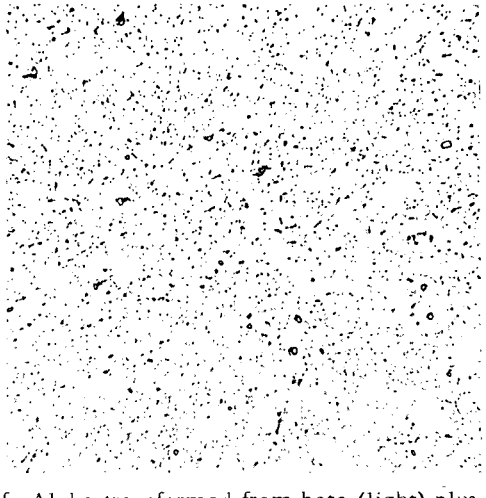

f. Alpha transformed from beta (light) plus very fine particles of delta (dark). Micro No. 17802.

All photomicrographs taken at 500X with bright field illumination. All specimens etched in phosphoric acid.

Figure 6. Microstructures of U-Zr Alloys Annealed in the α, $\alpha + \delta$, $\alpha + \gamma_2$, and $\beta + \gamma_2$ Phase Regions. (All alloys annealed 1 week at the indicated temperatures and water quenched.)

All photomicrographs taken at 500X with bright field illumination. All specimens etched in phosphoric acid.

U-0.4 w/o Zr 700°C

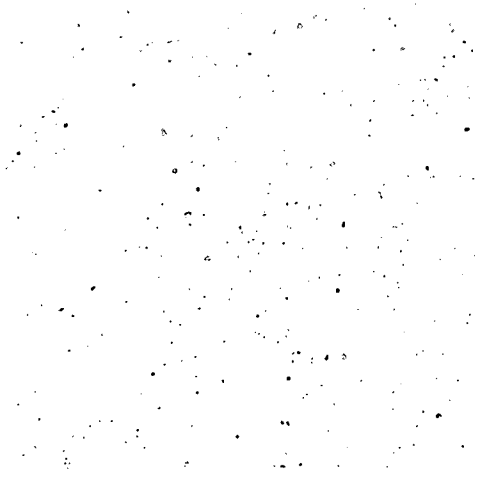

a. Micro No. 16982.

U-0.6 w/o Zr 700°C

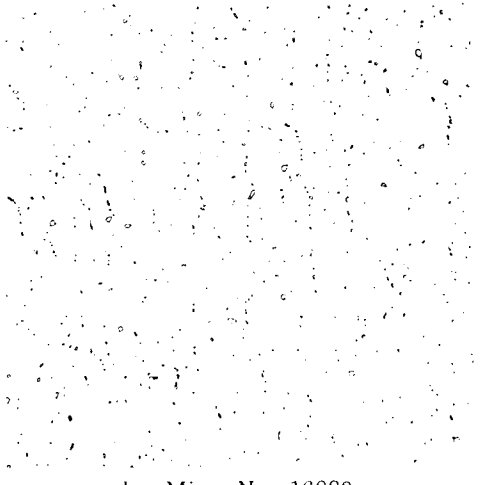

b. Micro No. 16983.

U-1.0 w/o Zr 700°C

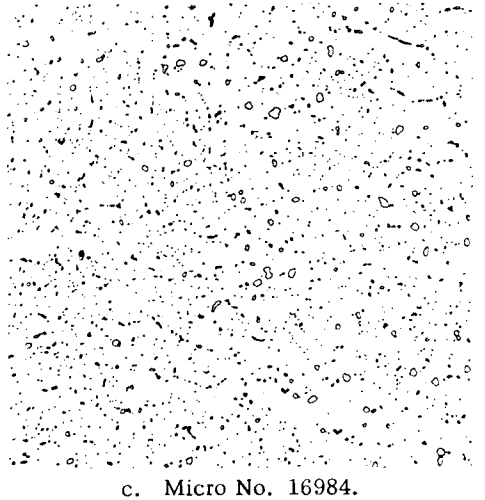

c. Micro No. 16984.

Small particles of martensitic alpha transformed from gamma1 in matrix of alpha transformed from beta.

U-0.4 w/o Zr 750°C

d. Micro No. 17776.

U-0.6 w/o Zr 750°C

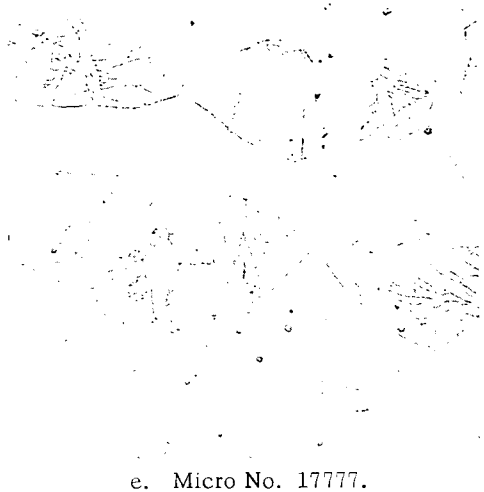

e. Micro No. 17777.

U-1.0 w/o Zr 750°C

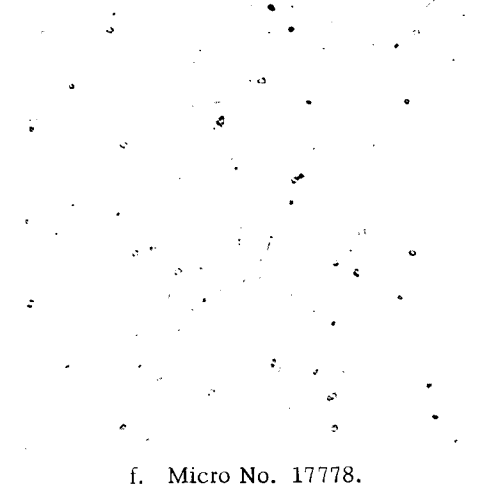

f. Micro No. 17778.

Martensitic alpha grains (acicular) in matrix of alpha transformed from beta. Angular particles are unidentified inclusions.

Figure 7. Microstructures of U-Zr Alloys Annealed in the $\beta + \gamma_1$ Phase Region. (Alloys annealed 1 week at the indicated temperatures and water quenched.)

From the data obtained, the solubility of zirconium in alpha uranium is placed at slightly in excess of 0.21 per cent at the beta eutectoid temperature, 662°C, and decreases with decreasing temperature to 0.09 per cent at 500°C. In beta uranium, maximum solubility is placed at slightly less than 0.41 per cent at the monotectoid reaction temperature, 693°C. The beta eutectoid composition is placed at 0.3 per cent zirconium.

The Eutectoid and Monotectoid Reactions

On heating a 1.0 per cent zirconium alloy at rates of the order of 1°C/min, thermal arrests were observed at 665°C, 694°C, and 752°C. The first two arrests, clearly associated with isothermal reactions, are related to the alpha-beta eutectoid and the monotectoid reactions, respectively. The temperatures of the reactions are in good agreement with those determined by Summers-Smith from dilatometric data: 662 ± 3°C and 693 ± 3°C, respectively. The third arrest at 752°C is associated with the $(\beta + \gamma_1)/\gamma_1$ reaction. On cooling at similar rates, arrests occurred at 723°C, 688°C, and 643°C. Despite the rather low rates of cooling, considerable hysteresis was observed for all three reactions, showing that the arrests that occur on cooling cannot be used for determining the true temperatures of the reactions. The cooling curve data are, however, significant in showing that all three reactions occur rather sluggishly.

The Gamma$_1$ plus Gamma$_2$ Phase Region

The temperature and compositional limits of the gamma$_1$ plus gamma$_2$ phase region were determined from metallographic studies of specimens annealed at 690°C, 700°C, 710°C, and 725°C and water quenched. The results of the studies are plotted in Figure 1.

All alloys containing from 4 to 23 per cent zirconium annealed at 690°C had microstructures showing that the beta and gamma$_2$ phases existed at the annealing temperature. In Figure 8 are photomicrographs illustrating the two-phase microstructures and as well the single-phase microstructures observed for alloys containing from 25 to 67 per cent zirconium, also annealed at 690°C within the gamma$_2$ region.

The two series of alloys annealed at 700°C and 710°C showed with changing zirconium composition a sequence of two-phase and single-phase microstructures. The sequence for the series annealed at 700°C is shown by the photomicrographs in Figure 9. At 4.0 per cent zirconium, the acicular martensitic product of the gamma$_1$ phase and alpha uranium transformed from beta are evident in the photomicrograph shown in Figure 9a. Figures 9b and 9c show only the martensitic product in alloys of 5.0 and 6.9 per cent zirconium. Figures 9d through 9g illustrate the microstructures of alloys annealed within the gamma$_1$ plus gamma$_2$ region.

All photomicrographs taken at 500X with bright field illumination

U-4.0 w/o Zr

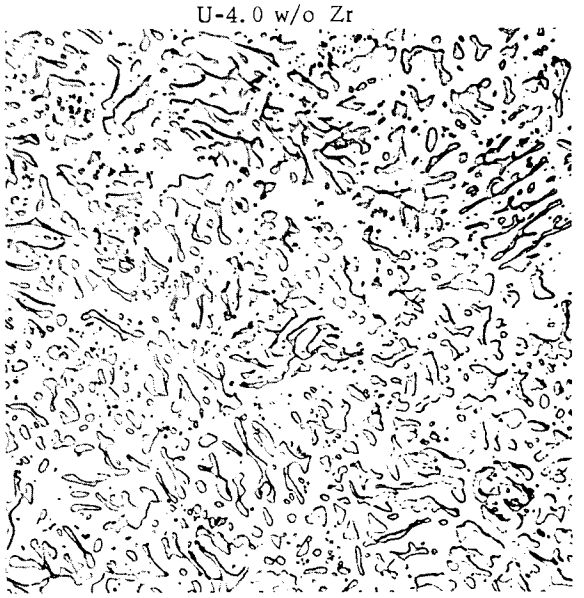

a. Alpha transformed from beta (light) plus spheroidal grains of supersaturated delta transformed from gamma$_2$. Etchant: Phosphoric Acid. Micro No. 20230.

U-14.0 w/o Zr

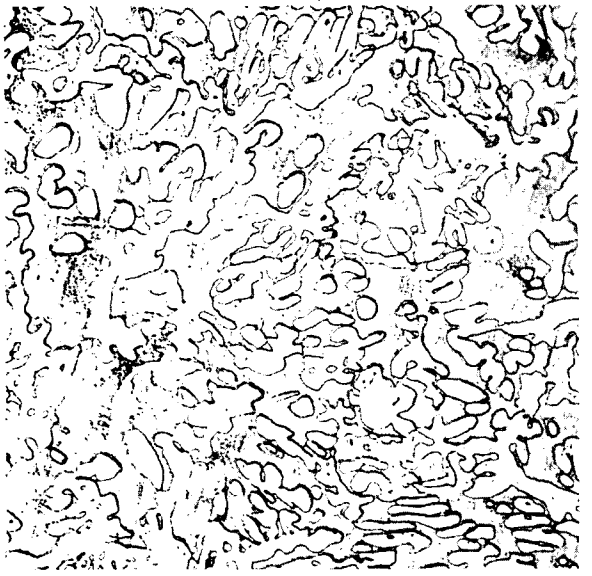

b. Supersaturated delta (grey) plus spheroidal grains of alpha (light). Etchant: Phosphoric Acid. Micro No. 20231.

U-23.0 w/o Zr

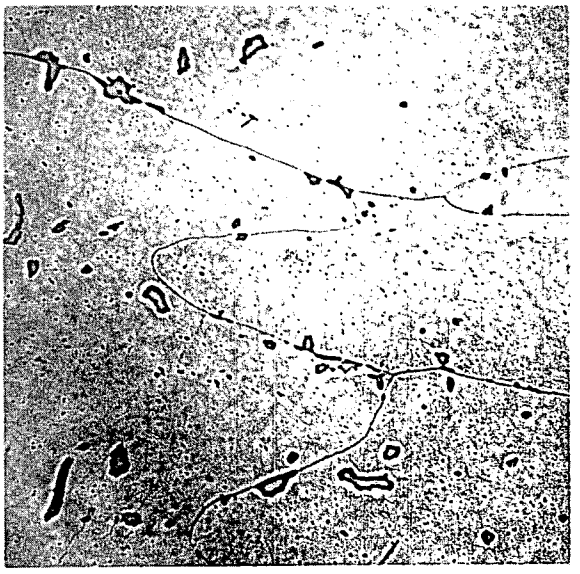

c. Coarse grain supersaturated delta plus small amount of alpha (dark grey). Etchant: Perchloric-Acetic Acids. Micro No. 20108.

U-25.0 w/o Zr

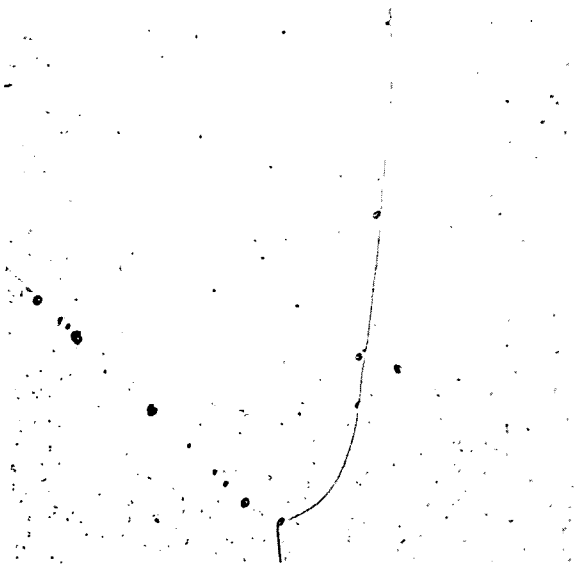

d. Metastable gamma containing small amount of inclusions. Etchant: Perchloric-Acetic Acids. Micro No. 20109.

Figure 8. Microstructures of U-Zr Alloys Containing 4.0 to 25.0 Per Cent Zr Annealed 1 Week at 690°C and Water Quenched.

U-4.0 w/o Zr

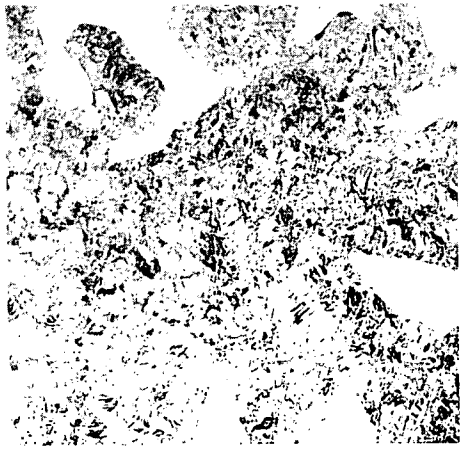

a. Martensitic alpha (acicular) transformed from gamma$_1$ plus supersaturated alpha (light) transformed from beta. Etchant: Phosphoric Acid. 500X. Micro No. 20194.

U-5.0 w/o Zr

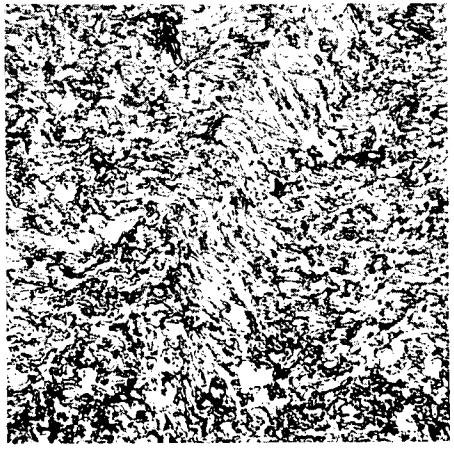

b. Martensitic alpha product of gamma$_1$. Etchant: Phosphoric Acid. 500X. Micro No. 20195.

U-6.9 w/o Zr (0-90 ppm)

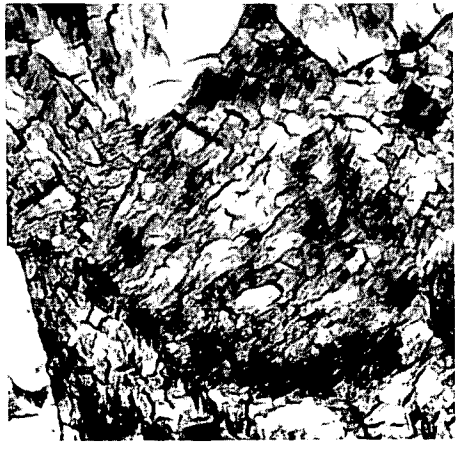

c. Martensitic alpha product of gamma$_1$. Etchant: Phosphoric Acid. 1000X. Micro No. 20196.

U-8.0 w/o Zr (0-150 ppm)

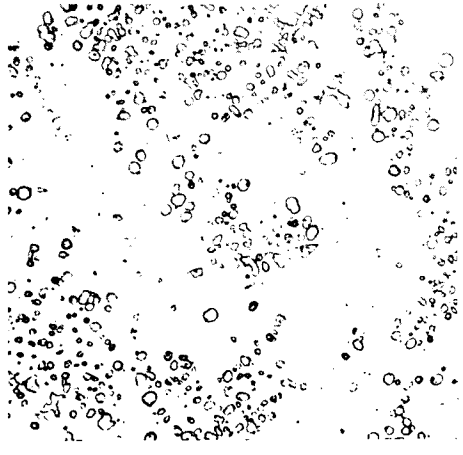

d. Martensitic alpha (light) plus particles of delta transformed from gamma$_2$. Etchant: Phosphoric Acid. 500X. Micro No. 20197.

U-14.0 w/o Zr

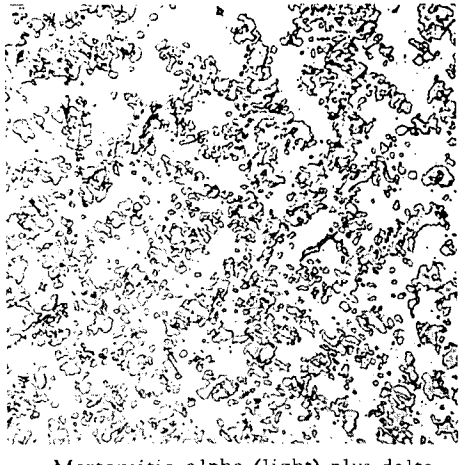

e. Martensitic alpha (light) plus delta transformed from gamma$_2$ (grey). Etchant: Phosphoric Acid. 500X. Micro No. 20201.

U-19.0 w/o Zr (0-110 ppm)

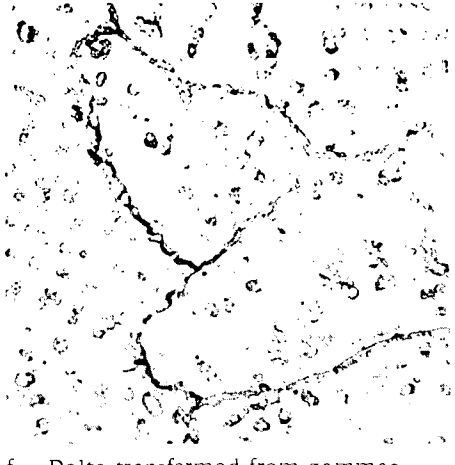

f. Delta transformed from gamma$_2$ (light) plus small amount of alpha (grey). Etchant: Perchloric-Acetic Acids. 500X. Micro No. 20199.

U-21.0 w/o Zr (0-55 ppm)

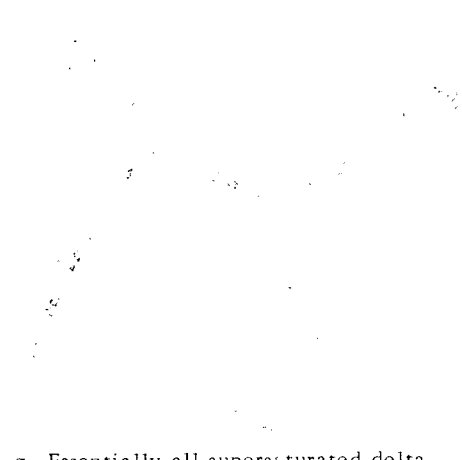

g. Essentially all supersaturated delta except for small amount of alpha in parent gamma$_2$ grain boundaries. Etchant: Perchloric-Acetic Acids. 500X. Micro No. 20200.

All photomicrographs taken with bright field illumination.

Figure 9. Microstructures of U-Zr Alloys Containing 4.0 to 21.0 Per Cent Zr Annealed 1 Week at 700°C and Water Quenched.

These consist of martensitic alpha transformed from $gamma_1$ and the delta phase transformed from $gamma_2$. Microstructures of alloys annealed within the two-phase region at 710°C were essentially the same as those of alloys annealed within the same region at 700°C. Microstructures of alloys annealed within the single-phase $gamma_2$ region at 700°C and 710°C resembled those of alloys annealed within the same region at 690°C (see Figure 8). From the observed microstructures the two-phase region, $gamma_1$ plus $gamma_2$ was determined to extend from 7.5 to 21.0 per cent zirconium at 700°C and from 9.5 to 19.0 per cent zirconium at 710°C.

In Figure 10 are photomicrographs illustrating the microstructures of the series of alloys annealed at 725°C. All alloys containing from 4 to 14 per cent zirconium show only the martensitic product related to $gamma_1$, as seen in Figure 10a. Between 14 and 21 per cent zirconium the martensitic reaction is, as previously noted, at 750°C gradually supplanted by the transformation of gamma to the delta phase. Figure 10b shows the coarse-grain delta-phase microstructure of a 21.0 per cent zirconium alloy. From these data, the peak of the $gamma_1$ plus $gamma_2$ phase region is determined to extend to some temperature below 725°C but above 710°C. Extrapolation of the compositional limits determined for the region at 700°C and 710°C places the peak at 722°C and 14 per cent zirconium. Similar extrapolation of the $(\beta + \gamma_1)/\gamma_1$ boundary and the $\gamma_1/(\gamma_1 + \gamma_2)$ boundary places the monotectoid composition at 4.5 per cent zirconium.

U-14.0 w/o Zr (0-50 ppm)

a. Acicular martensitic alpha transformed from $gamma_1$. Etchant: Phosphoric Acid. Bright Field. 500X. Micro No. 20227.

U-21.0 w/o Zr (0-52 ppm)

b. Supersaturated delta transformed from $gamma_2$. Etchant: Perchloric-Acetic Acids. Bright Field. 500X. Micro No. 20228.

Figure 10. Microstructures of U-14.0 Per Cent Zr and U-21.0 Per Cent Zr Alloys Annealed 1 Week at 725°C and Water Quenched.

After microexamination, chemical analyses for oxygen were obtained for several selected specimens of the series annealed at 700°C and 725°C. The results of the analyses, given in Table II, show oxygen concentrations ranging in general from 36 to 150 ppm. This level is consistent with that determined for the as-cast condition (see Table I); these results indicated that little or no contamination occurred during annealing.

In earlier work with evacuated rather than argon-filled annealing capsules, two similar series of specimens were annealed at the same temperatures, 700°C and 725°C. Chemical analyses of these specimens after annealing showed oxygen concentrations ranging generally from 160 to 355 ppm, as seen in Table II. The influence of these higher oxygen concentrations upon microstructures was found to be quite marked, as can be seen from comparison of the photomicrographs in Figures 9 and 10 with those in Figures 11 and 12. Alloys which are clearly seen to be either single-phase gamma$_1$ or gamma$_2$ at low oxygen concentrations are two phase at the higher oxygen levels. It is concluded from this that oxygen concentrations within the range from 160 to 355 ppm are in excess of the maximum solubility limits of oxygen in the gamma phases.

Table II

OXYGEN CONCENTRATIONS IN ANNEALED U-Zr ALLOYS

Annealing Treatment	Alloy No.	Nominal w/o Zr	Oxygen (ppm)
One week in pressurized (argon) capsules at 700°C and water quenched	11	6.9	90
	12	8.0	150
	21	19.0	110
	22	21.0	55
One week in pressurized (argon) capsules at 725°C and water quenched	9	5.0	36
	18	14.0	50
	22	21.0	52
Three weeks in evacuated capsule at 700°C and water quenched	10	6.5	270
	11	6.9	251
	23	21.3	195
	24	23.0	355
Three weeks in evacuated capsule at 725°C and water quenched	9	5.0	115
	16	11.4	160
	23	21.3	251

All photomicrographs taken at 500X with bright field illumination

U-5.0 w/o Zr

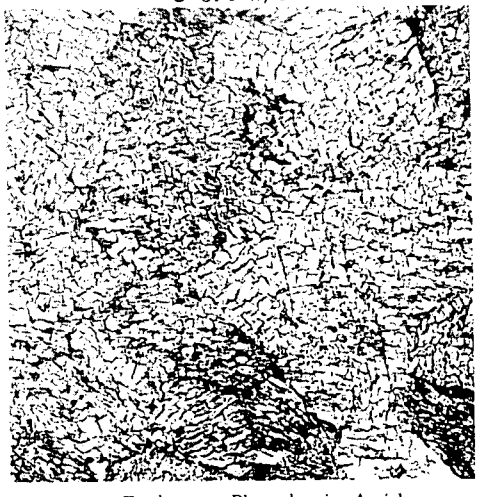

a. Etchant: Phosphoric Acid.
Micro No. 20113.

U-6.5 w/o Zr (0-270 ppm)

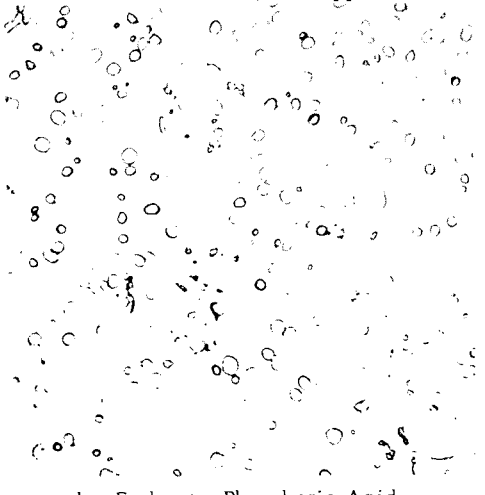

b. Etchant: Phosphoric Acid.
Micro No. 20114.

U-6.9 w/o Zr (0-251 ppm)

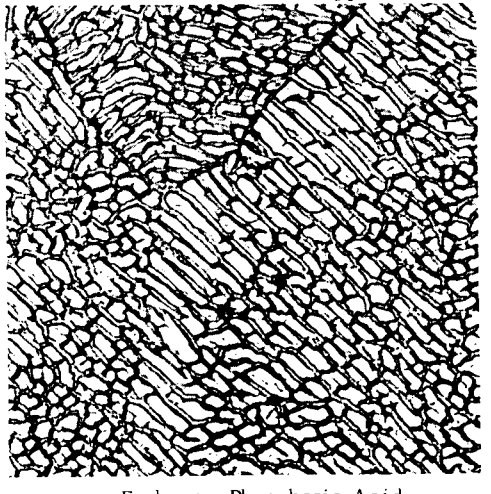

c. Etchant: Phosphoric Acid.
Micro No. 20115.

U-21.3 w/o Zr (0-195 ppm)

d. Etchant: Perchloric-Acetic Acids.
Micro No. 20118.

U-23.0 w/o Zr (0-355 ppm)

e. Etchant: Perchloric-Acetic Acids.
Micro No. 20119.

U-32.0 w/o Zr

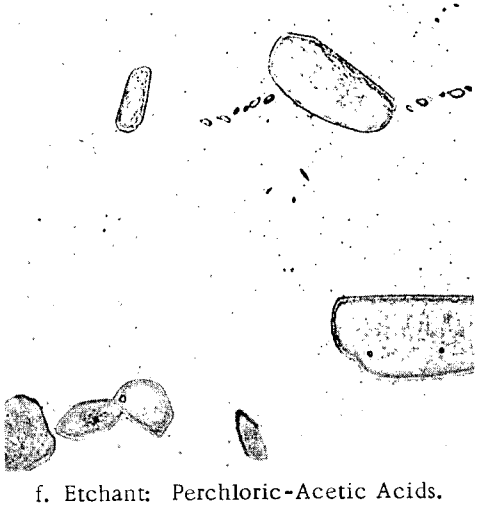

f. Etchant: Perchloric-Acetic Acids.
Micro No. 20122.

Figure 11. Microstructures of U-Zr Alloys Containing High Oxygen Concentrations Annealed 3 Weeks at 700°C and Water Quenched.

All photomicrographs taken at 500X with bright field illumination

U-5.0 w/o Zr (0-115 ppm)

a. Etchant: Phosphoric Acid.
Micro No. 20234.

U-6.5 w/o Zr

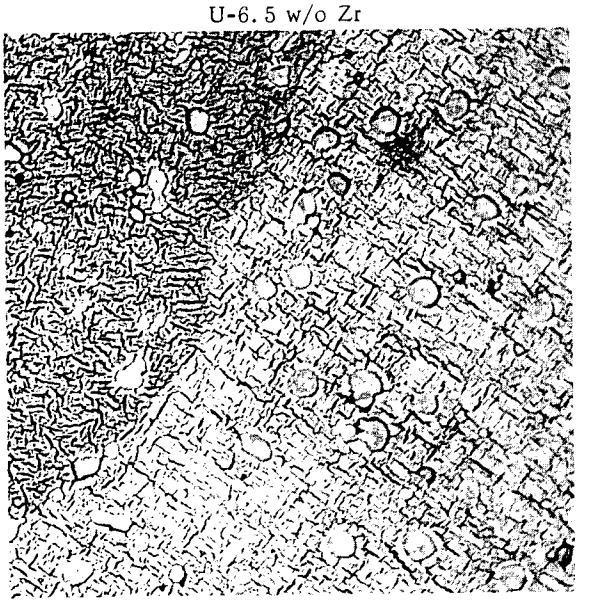

b. Etchant: Phosphoric Acid.
Micro No. 20235.

U-11.4 w/o Zr (0-160 ppm)

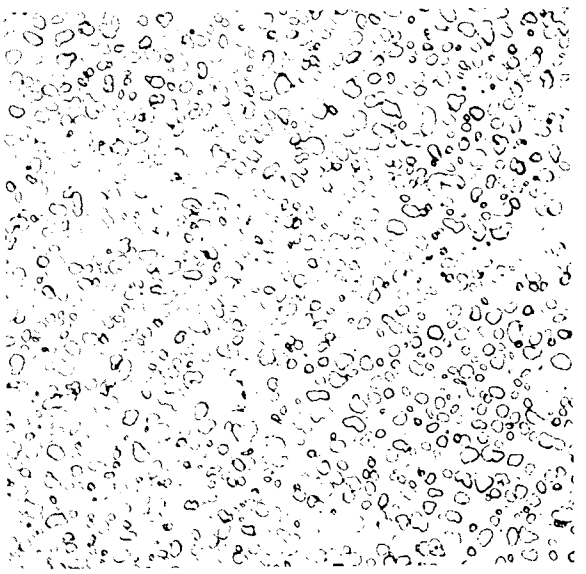

c. Etchant: Phosphoric Acid.
Micro No. 20238.

U-21.3 w/o Zr (0-251 ppm)

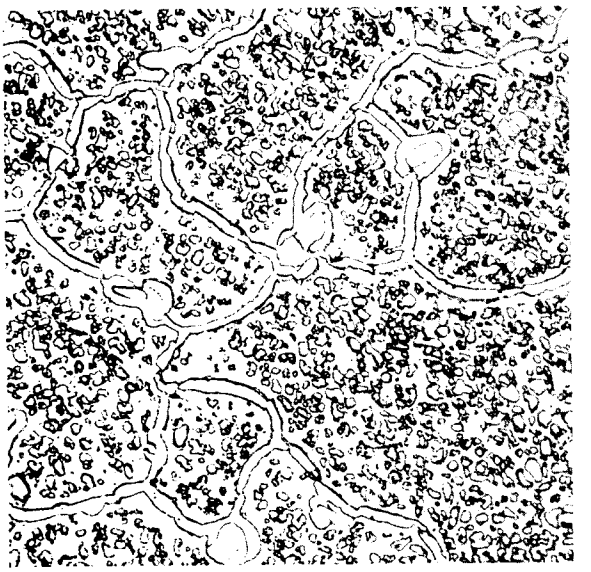

d. Etchant: Phosphoric Acid.
Micro No. 20239.

Figure 12. Microstructures of U-Zr Alloys Containing High Oxygen Concentrations Annealed 3 Weeks at 725°C and Water Quenched.

The phases coexisting with the oxygen saturated gamma phases at 700°C and 725°C and appearing in the microstructures shown in Figures 11 and 12 were not determined in this investigation. Thus it is not possible to define rigorously the influence of the higher oxygen concentrations on phase relations in the area of the miscibility gap. The fact that two phases occur at the higher oxygen levels suggests, however, that in the U-Zr-O ternary system the miscibility gap does not disappear in favor of a single-phase gamma solid solution region as is the case in the U-Zr-Ti system.[16] Instead, it appears that either the gap is expanded in the ternary system, as earlier reported,[17] or that it is replaced by phase regions in which oxygen-saturated gamma phases, either $gamma_1$ or $gamma_2$, occur in equilibrium with oxygen-rich phases. In view of these observations it is seen that the boundaries of the $gamma_1$ plus $gamma_2$ region shown in Figure 1 apply only to alloys containing oxygen in amounts not greater than 150 ppm.

SUMMARY

The solubilities of zirconium in alpha and beta uranium were determined from metallographic studies of annealed and quenched alloys. In alpha uranium, maximum solubility is placed at slightly in excess of 0.21 weight per cent at 662°C and is shown to decrease to 0.09 weight per cent at 500°C. In beta uranium, maximum solubility is placed at slightly less than 0.41 weight per cent at 693°C. The beta eutectoid composition is placed at 0.3 weight per cent zirconium. Thermal arrest data obtained on heating an U-1.0 weight per cent zirconium confirm the temperatures 693°C for the $gamma_1$ monotectoid reaction, and 662°C for the beta eutectoid reaction, earlier established by Summers-Smith.[14]

From metallographic studies of U-Zr alloys containing less than 150 ppm of oxygen by weight, the $gamma_1$ plus $gamma_2$ phase region boundaries were determined to be 4.5 weight per cent and 22.0 weight per cent at the monotectoid reaction temperature. The peak of the region is placed at 722°C and 14 weight per cent zirconium on extrapolation of compositional limits determined for 700°C and 710°C. A revised phase diagram of the uranium-zirconium alloy system in which the above described features are incorporated is shown in Figure 1.

Metallographic data are presented which show that phase relations in the area of the $gamma_1$ plus $gamma_2$ phase region are influenced significantly by oxygen in amounts ranging from 160 to 355 ppm by weight.

ACKNOWLEDGMENTS

The author wishes to acknowledge gratefully the help of P. Beck of the University of Illinois, and of M. V. Nevitt, H. H. Chiswik, and L. T. Lloyd of Argonne National Laboratory in all phases of this work. Thanks are due to M. Mueller for assistance in X-ray diffraction work and to R. P. Wilhelmi for assistance in the preparation of alloys and metallographic studies. The author also wishes to thank F. A. Rough and A. A. Bauer, and D. Summers-Smith for permission to reproduce their proposed equilibrium phase diagrams of the uranium-zirconium alloy system.

BIBLIOGRAPHY

1. Rough, F. A., and Bauer, A. A., Constitutional Diagrams of Uranium and Thorium Alloys, Addison-Wesley Pub. Co., Reading, Mass. (1958).

2. Kaufman, A. R., Technical Progress Report, MIT-1078 (April 1952).

3. Peterson, D., Quarterly Summary Research Report in Metallurgy, ISC-575 (July 1955).

4. Buzzard, R. W., Liss, R. B., and Fickle, D. P., The Uranium-Zirconium Binary System, J. Met. and Ceramics, TID-2002 (Aug 1952).

5. Bauer, A. A., Beatty, G. H., and Rough, F. H., The Constitution of Zirconium-Uranium Alloys Containing Oxygen or Nitrogen, Trans. A.I.M.E., 212, 801-807 (Dec 1958).

6. Rough, F. A., Austin, A. E., Bauer, A. A., and Doig, J. R., The Stability and Existence Range of the Zirconium-Uranium Epsilon Phase, BMI-1092 (May 1956).

7. Holden, A. N., and Seymour, W. E., The Uranium-Zirconium System, Trans. A.I.M.E., 209, 515 (1957).

8. Duffy, J. F., and Bruck, C. A., The Delta Phase Field of the Uranium-Zirconium Equilibrium Diagram, Trans. A.I.M.E., 212, 17-19 (Feb 1958).

9. McGeary, R. K., Dilatometric Investigation of Zirconium, Zirconium-Uranium, Zirconium-Oxygen and Zirconium-Nitrogen Alloys, WAPD-36 (July 1951).

10. Mueller, M. H., The Delta Phase Found in U-Zr Alloys, Acta Cryst., 8, 849-850 (1955).

11. Silcock, J. M., Trans. A.I.M.E., 209, 521 (1957).

12. Boyko, E. R., The Structure of the Phase in the Uranium-Zirconium System, Acta Cryst., 10, 712 (1957).

13. Mueller, M. H., Knott, H. W., and Heaton, L., The Hexagonal Phase Found in Certain Zirconium and Titanium Alloys, Presented at the 15th Pittsburgh Diffraction Conference, November 7, 1957.

14. Summers-Smith, D., The Constitution of Uranium-Zirconium Alloys, J. Inst. Metals, 83 (Feb 1955).

15. Zegler, S. T., and Terandy, J., Multiple Crucible Arc Melting Furnace, Metal Prog., 70, 116 (1956).

16. Howlett, B. W., The Alloy System Uranium-Titanium-Zirconium, J. Nuclear Materials, 3, 289-299 (1959).

17. Chiswik, H. H., Dwight, A. E., Lloyd, L. T., Nevitt, M. V., and Zegler, S. T., Advances in the Physical Metallurgy of Uranium and its Alloys, Proceedings of the United Nations Second International Conference on the Peaceful Uses of Atomic Energy, Geneva, Switzerland 6, 394-412 (1958).